HHS Public Access

Author manuscript

J Cell Physiol. Author manuscript; available in PMC 2020 February 01.

Published in final edited form as:

J Cell Physiol. 2019 February ; 234(2): 1671–1681. doi:10.1002/jcp.27037.

Irisin promotes cardiac progenitor cell-induced myocardial repair and functional improvement in infarcted heart

Yu Tina Zhao[1,#], **Jianguo Wang**[1,#], **Naohiro Yano**, **Ling X Zhang**[2], **Hao Wang**[1], **Shouyan Zhang**[3], **Gangjian Qin**[4], **Patrycja M Dubielecka**[2], **Shougang Zhuang**[2], **Paul Y Liu**[5], **Y Eugene Chin**[6], and **Ting C Zhao**[1,*]

[1]Department of Surgery, Roger Williams Medical Center, Boston University School of Medicine

[2]Department of Medicine, Rhode Island Hospital, Brown University, Providence, RI

[3]Department of Medicine, Luoyang Central Hospital, Zhengzhou University, Luoyang, China

[4]Department of Biomedical Engineering, University of Alabama at Birmingham, Birmingham, Alabama

[5]Department of Plastic Surgery, Rhode Island Hospital, Brown University, Providence, RI

[6]Institute of Health Sciences, Chinese Academy of Sciences-Jiaotong University School of Medicine, Shanghai, China

Abstract

Irisin, a newly identified hormone and cardiokine, is critical for modulating body metabolism. New evidence indicates that irisin protects the heart against myocardial ischemic injury. However, whether irisin enhances cardiac progenitor cell-induced cardiac repair remains unknown. This study examines the effect of irisin on cardiac progenitor cell (CPC)-induced cardiac repair when these cells are introduced into the infarcted myocardium. Nkx 2.5^+ CPC stable cells were isolated from mouse embryonic stem cells. Nkx 2.5^+CPCs (0.5×10^6) were re-introduced into the infarcted myocardium using PEGylated fibrin delivery. The mouse MI model was created by permanent ligation of the left anterior descending artery (LAD). Nkx 2.5^+CPCs were pretreated with irisin at a concentration of 5 ng/mL *in vitro* for 24 hours prior to transplantation. Myocardial functions were evaluated by echocardiographic measurement. Eight weeks after engraftment, Nkx 2.5^+ CPCs improved ventricular function as evident by an increase in ejection fraction (EF) and fractional shortening (FS). These findings are concomitant with the suppression of cardiac hypertrophy and attenuation of myocardial interstitial fibrosis. Transplantation of Nkx 2.5^+ CPCs promoted cardiac regeneration and neovascularization, which were increased with the pretreatment of Nkx 2.5^+ CPCs with irisin. Furthermore, irisin treatment promoted myocyte proliferation as indicated by proliferative markers Ki67 and phosphorylated histone 3 and decreased apoptosis. Additionally, irisin resulted in a marked reduction of HDAC4 and increased p38 acetylation in cultured CPCs. These results indicate that irisin promoted Nkx 2.5^+ CPC-induced cardiac

[*]Corresponding Author: Ting C Zhao, MD, Associate Professor, Department of Surgery,, Boston University Medical School,, Roger William Medical Center, 50 Maude Street, Providence, RI 02908, tzhao@bu.edu, Fax: 401-456-2507, Tel: 401-456-8266.
[#]Equal contribution

Conflict of interests:
The authors declare that they have no competing interests.

regeneration and functional improvement and that irisin serves as a novel therapeutic approach for stem cells in cardiac repair.

Keywords

Irisin; Cardiac progenitor cell; myocardial infarction; Ventricular function

Background

Despite rapid advancements in both pharmacological and interventional treatment options, ischemic heart disease is the leading cause of morbidity and mortality worldwide (Finegold JA et al., 2013). The quest for new therapeutic approaches to prevent adverse myocardial remodeling post-infarction and limit the subsequent development of irreversible heart failure gave rise to the field of stem cell therapy (Stamm C et al., 2003). Earlier attempts to treat MI have employed various stem cells, including hematopoietic stem cells, mesenchymal stem cells, and embryonic stem cells (Stamm C et al., 2003; Qiao H et al., 2011; Zhang S et al., 2005; Zhao M et al., 2005). It has now been recognized that adult hearts harbor distinct populations of cardiac progenitors (Musunuru K et al., 2010), which have the potential to differentiate into cardiomyocytes, endothelia, and vascular smooth muscle cells. Furthermore, several studies have shown that these cardiac progenitor cells are capable of differentiating into cardiac tissue and improving cardiac function after myocardial injury (Zhang LX et al., 2014; Oh H et al., 2003; Laugwitz KL et al., 2005). These new findings led to a novel understanding of both normal and pathologic cardiac developments and homeostasis, and foster a transition towards therapeutic goals for cardiac regenerative medicine. Recent studies have investigated the role of cardiac progenitor cells (CPCs) as the specific regenerative cell source of the heart, which has opened a new approach for cell-based cardiac repair therapy (Menasché P et al., 2015). However, CPC therapy has limitations resulting from poor cell viability after transplantation (Westrich J et al.,2010). Strategies to improve cell survival and reduce cell apoptosis are necessary if the potential of CPC therapy is to be fulfilled.

Irisin is a recently identified proliferator-activated receptor-gamma coactivator-1α (PGCγ-1α)-dependent myokine, and is secreted by skeletal muscle and myocardium into circulation during exercise as a cleavage product of the extracellular portion of type I membrane protein fibronectin type III domain containing 5 (FNDC5) (Zhang L et al., 2012). It was initially discovered as a hormone responsible for the beneficial effects of exercise on the browning of white adipose tissues and increases in energy expenditure (Boström P et al., 2012). It has also been demonstrated to reduce oxidative stress and apoptosis in different models (Park MJ et al., 2015; Zhu D et al., 2017). Recent evidence has indicated that irisin could induce the browning of white adipose tissue, which could be used as a therapeutic tool for metabolic disorders and cardiovascular diseases (Jeremic N et al., 2017). In an apoE$^{(-/-)}$ diabetic mouse model, the systemic administration of irisin protected against endothelial injury and ameliorated atherosclerosis, indicating that irisin could be therapeutic for atherosclerotic vascular diseases in diabetes (Lu J et al., 2015). Additionally, decreased

serum and vitreous irisin concentrations were found in type 2 diabetes mellitus patients (Hu W et al., 2018).

Recently, we presented cardioprotective effects of irisin against myocardial ischemia/reperfusion injury and hypoxia/re-oxygenation injury through the activation of MAP kinases and the preservation of mitochondrial function in cardiomyoblasts and the heart (Wang H et al., 2017; Zhao YT et al., 2016). However, the functional role of irisin on promoting Nkx2.5 CPC-derived regeneration has yet to be thoroughly investigated. Therefore, we pretreated CPCs with irisin before delivering them into infarcted areas of hearts to determine if the myokine showed beneficial effects on the recovery of the CPC transplanted heart from ischemic damages. Our results demonstrate that irisin plays a pivotal role in directing CSCs to promote cardiac repair when introduced into an MI heart.

Methods

Animals

All studies on animals were performed under a protocol approved by the Institutional Animal Care and Use Committee, which conforms to the Guide for the Care and Use of Laboratory Animals published by the US National Institutes of Health (NIH Publication No. 85–23, revised 1996); these animals were housed in an accredited facility of Roger Williams Medical Center (Providence, RI, USA). All animal procedures were carried out in accordance with guidelines approved by the Institutional Animal Care and Use Committee of Roger Williams Medical Center. CD-1 mice were purchased from Charles River Laboratories (Wilmington, MA) and housed at the Animal Care Facility of Roger Williams Medical Center on a 12-hour light/dark cycle with free access to water and standard mouse food.

Isolation and preparation of stable Nkx2.5$^+$ CPCs

Mouse embryonic stem cells (CGR8, generation 12-14; Sigma Aldrich, St. Louis, MO, USA) were cultivated in gelatin-coated petri-dishes in Dulbecco's Modified Eagle's Medium (DMEM) supplemented with 1× non-essential amino acids, 100 μg/mL penicillin, 100 U/mL streptomycin, 2 mM L-glutamine, 0.1 mM β-mercaptoethanol, 1 mM sodium pyruvate, 15 % fetal bovine serum, and 10^3 U/ml leukemia inhibitory factor (LIF). Cells were maintained at 37°C in a humidified atmosphere with 5% CO_2. Monolayered cells were dissociated using 0.05% Trypsin/EDTA (Invitrogen, Carlsbad, CA, USA) and 5 ×10^6 cells were resuspended and transfected with linearized Nkx2-5.Hsp68.PAC plasmid (FspI) using Lipofectamine 2000 (Invitrogen). The transfected cells were maintained under pressure with 500 μg/L of G418 for at least two weeks until large undifferentiated clonal colonies became clearly visible. After the initial selection, stable Nkx2.5$^+$CPC-positive colonies were established and picked up under fluorescent microscopy, and were subjected to cell culture conditions for subcultures to expand. After establishing Nkx2.5$^+$CPC, some portion of the cells was exposed to irisin (5ng/ml) for 24 hours to induce preconditioning of Nkx2.5$^+$CPCs, which is an established protective approach. The dose of irisin was established here, which is based on a study in which this concentration of irisin induced a protective effect in embryonic rat cardiomyoblasts exposed to hypoxia/reoxygenation (Zhao YT et al., 2016). In

addition, to determine whether irisin treatment could induce the apoptosis of Nkx2.5 CPCs, we further examined the content of apoptosis of Nkx2.5 CPCs following irisin treatment as described before (Chen HP et al., 2011). In brief, Nkx2.5 CPCs were pretreated for 1 h with the following: 1) control; 2) irisin (5ng/ml) before cells were exposed to 100 μmol/L hydrogen peroxide for 2 h and resumed with culture medium for 1 h. The protein was extracted and subjected to analysis of active caspase-3 signals.

PEGylated fibrin gel delivery of Nkx2.5$^+$ CPCs

CPCs were infected with eGFP adenovirus (Vector Biolabs, Inc, Philadelphia, PA) following previously established methods, and then were injected into the infarcted ventricular myocardium. In order to increase the delivery of engrafted cells following cell injection in the infarcted myocardium, we used a PEGylated fibrin approach for stable Nkx2.5$^+$ CPC engraftment in the study (Zhang G et al., 2006); this could provide a biomimetic environment for cell growth as other approaches (Zhang D et al., 2010). PEGylated fibrin injections were prepared by combining bifunctional PEG succinimidyl glutarate (4 mg/mL in PBS without calcium; NOF America) with human fibrinogen (10 mg/mL in PBS, Sigma-Aldrich) in a 1:1 volume ratio. An equal volume of CPCs was mixed with the PEGylated fibrin solution in a 1:1 volume ratio at a concentration of 0.5×10^5 cells/μl. The solution was then loaded into a G28 needle syringe with an equal volume of thrombin (200 U/mL in 40 mM $CaCl_2$). The solution was mixed thoroughly within the syringe and the gel solution (20 μL) for an injection to infarcted areas of the myocardium.

Myocardial Infarction

Two-month old male ICR (CD-1) mice were obtained from Charles River Laboratories (Wilmington, MA, USA). The mouse myocardial infarction model was created following thoracotomy by applying permanent ligation to the left anterior descending (LAD) artery as previously described (Zhang LX et al., 2014). Briefly, mice were anesthetized by an intraperitoneal injection of 50 mg/kg sodium pentobarbital. Mice received a subcutaneous injection of buprenorphine (0.03 mg/kg) 2 hr before surgery and also every 12 hr post-surgery for 3 days. Ventilation was achieved by connecting the endotracheal tube with a rodent ventilator (Model 683; Harvard Apparatus, Holliston, MA, USA). The chest was then opened, and coronary occlusion was induced by ligation with a nylon suture. Mice in the sham (Sham) group were anesthetized and underwent thoracotomy without coronary ligation.

In vivo cell transplantation into MI heart

Upon completion of the LAD ligation, a total of 5×10^5 GFP-labeled Nkx2.5$^+$ CPCs suspended in 20 μl of PEGylated fibrin solution was directly injected into five sites in the border zones of the infarcted left ventricles, which is shown in Supplemental Figure 1. Mice in the MI-Nkx2.5$^+$ CPC$^+$ group received control Nkx2.5$^+$ CPC (MI + CPC group), while MI-Nkx2.5$^+$ CPC + Irisin group mice received irisin-treated Nkx2.5$^+$ CPC (MI + CPC + Irisin group). The MI group received CPC free vehicle (PBS). Following Nkx2.5$^+$ CPC injections, the chest was closed by a 5-0 Tricon suture with one layer through the chest wall and muscle and a second layer through the skin and subcutaneous material, followed by air

evacuation to prevent pneumothorax. Mice were sacrificed at 8 weeks after operation to obtain heart tissues for evaluations.

Echocardiography

Echocardiography of mice was conducted just before sacrifice using an Acuson Sequoia C512 system equipped with a 15L8 linear array transducer to access LV function. Mice were anesthetized with 1.5% isoflurane mixed with oxygen via a nose cone, and then placed in the supine position on a heating pad. After removal of hair, the precordial region was covered with pre-warmed ultrasound transmission gel (Aquasonic, Parker Laboratory, Fairfield, NJ). Short axis measurements were used to capture M-mode tracing at the level of the papillary muscles. The signal depth was set to 25mm. Three to six consecutive cardiac cycles were measured from M-mode tracings with accompanying software. All measurements were performed by a single experienced operator blinded to the mouse genotypes.

Histological analysis

Paraffin embedded heart tissue slices were fixed with 10% neutral buffered formalin and washed twice with PBST. Myocyte cross-sectional area was measured from images captured from the sections obtained mid-distance from the base to the apex. The outline of myocytes was traced using NIH Image J software (NIH, version 1.40g, http://rsb.info.nih.gov/ij/) to determine myocyte cross-sectional area. A value from each heart was calculated by the measurements of ~400–600 cells in remote and border areas from infarction of an individual heart. To evaluate cardiac fibrosis, LV sections were stained with picrosirius red, and collagen content was quantitated in images taken under a microscope coupled to a computerized morphometry system (Olympus BX41). Interstitial collagen density was expressed as a percentage per field (%) in each image. For immunofluorescent staining, fixed slices were incubated with appropriate primary antibodies overnight at 4°C. Primary antibodies used in this study were as follows: anti-troponin C (MS-295-P, Thermo-Fisher Scientific), anti-SMA (A5228, Sigma Aldrich), anti-WGA (L4895, Sigma Aldrich), anti-CD31 (CBL1337, Millipore), anti-phospho-histone 3 (07-145, Millipore), anti-Ki67 (NCL-Ki67p, Leica Biosystems Inc.), and anti-caspase 3 (ab13847, Abcam). After washes with PBS-T (3×5 min), the slides were incubated with Alexa Fluor 488 goat anti-mouse IgG (A11001, Invitrogen), Alexa Fluor 555 goat anti-rabbit IgG (A21428, Invitrogen), or Alexa Fluor 555 goat anti-rat IgG (A21434, Invitrogen) secondary antibodies (1:2000) for 2 hrs at room temperature in the dark. Then, the slides were washed (5×5 min), and DAPI containing mounting medium was applied. Confocal fluorescent microscopy was performed using a Carl Zeiss LSM 700 laser scanning microscope equipped with intuitive ZEN 2009 software. 5-10 randomly selected high-power fields were selected for quantification using Image J software. In addition, for immunostaining of cultured $Nkx2.5^{+}$ CPCs, cells were fixed in 4% paraformaldehyde for immunocytochemical analysis using rabbit anti-Nkx2.5 (diluted 1:200) for examination of Nkx2.5, a transcriptional factor of cardiac progenitor cells. Fluorescent signal was detected with Alexa Fluor 555 goat anti-rabbit IgG, which was shown in Supplemental Figure 2.

Terminal deoxynucleotidyl transferase mediated dUTP nick end labeling assay (TUNEL)

Paraffin embedded sections were fixed with 10% neutral buffered formalin and processed as above. Survival of transplanted cells was detected on the sections above with TUNEL labeling using TACS® 2 TdT Fluorescein Kit from Trevigen (Gaithersburg, MD) following the manufacturer's instructions. Nuclei were stained with DAPI and myocytes were labeled with troponin T. TUNEL positive signals were captured in the border area of the infarcted myocardium. The numbers of TUNEL positive nuclei were observed using confocal laser scanning microscopy, determined, and normalized to the percentage of total nuclei.

Western blot

The methods and details for protein preparations, immunoprecipitation, and immunoblotting were conducted as previously described (23). Briefly, the blots were incubated with polyclonal antibodies, including p38, HDAC4, anti-lysine polyclonal, and β-actin monoclonal antibodies at a dilution concentration of 1:1,000 and then visualized by using anti-rabbit or anti-mouse horseradish peroxidase-conjugated secondary antibody (1:2,000). Lastly, the blots were developed using ECL chemiluminescence detection reagent (Amersham Pharmacia Biotech).

Statistical analysis

Data were expressed as an average ± SEM of at least three independent experiments. An unpaired, two-tailed Student t-test was used to determine significance. Multiple treatments were analyzed using one-way ANOVA followed by Bonferroni post hoc test. Differences between groups were considered statistically significant when $p < 0.05$.

Results

Irisin pre-treatment improves cardiac function of CPC transplanted LAD ligated mice

To investigate whether the preservation of LV function by CPC transplantation was improved by irisin treatment, echocardiographic measurements were performed eight weeks after engraftment. There is no significant difference in ventricular function prior to surgical operation among the groups (Table 1). As shown in Figure 1a, left ventricular ejection fraction (EF) after LAD ligation significantly decreased following myocardial infarction. Myocardial function was improved by CPC transplantation in MI hearts (68.88% ± 1.48, 32.73% ± 3.49 and 44.24% ± 3.10, sham, MI Control, and MI + CPC, respectively). Notably, pre-treatment of CPCs with irisin significantly enhanced the improvement of CPC-induced ventricular function (54.94% ± 1.75, $p<0.01$ vs. MI + CPC). Likewise, left ventricular fractional shortening (FS) also manifested improvement following the treatment of CPCs (Figure 1a). Representative images of M-mode among groups are shown in Figure 1b. CPC treatment resulted in the reduction of LVIDd and LVIDs in comparison to the MI only group (Figure 1c and d). However, irisin treatment of CPCs did not attenuate the magnitude of LVIDs and LVIDd as compared to CPC+MI group.

Irisin pre-treatment promotes *in vivo* differentiation of CPCs into cardiomyocytes and smooth-muscle cells of vessels

CSC-derived cardiomyocytes were identified by double positive staining of GFP and troponin T within the infarct sites of the CPC-engrafted MI heart. As shown in Figures 2a and c, the number of the CPC-derived cardiomyocytes in infarcted areas were significantly increased by twofold in the MI + CPC + Irisin group in comparison to the MI + CPC group (1.93± 0.26 and 4.00 ± 0.36 per field, MI + CPC and MI + CPC + Irisin, respectively, $p < 0.001$). Newly formed microvessels were determined with GFP/α-SMA staining. CPC-derived smooth-muscle vessels also increased almost twofold in the MI + CPC + Irisin group (7.20 ± 0.85 and 14.06 ± 1.35 per field, MI + CPC and MI + CPC + irisin, respectively, $p < 0.001$, Figure 2b and d). In addition, the retained CPCs were increased by using PEGylated fibrin gel delivery of CPCs (Supplemental Figure 3).

Irisin treatment attenuated anti-remodeling effect of CPC transplantation in the post-MI heart

Wheat germ agglutinin staining was performed to measure the size of cardiomyocytes close to the infarct border of each group. As shown in Figure 3a and b, there is a significant increase in cross-sectional cardiomyocyte diameters in MI mice as compared with mice in the sham group. Cardiomyocyte hypertrophy that was demonstrated in MI hearts was suppressed by transplantation of CPCs (357.44 ± 5.90, 578.51± 11.53, and 509.88 ± 11.28μm^2 cross sectional area, sham, MI and MI + CPC group, respectively). Likewise, this anti-hypertrophic effect of CPC transplantation was more apparent in the MI + CPC + Irisin group (431.29 ± 6.34μm^2 cross sectional area, $p< 0.001$ vs. MI + CPC group).

Irisin pre-treatment promotes angiogenesis in cardiac tissue after ischemic injury

To assess the angiogenic response in post-MI hearts, we measured the vascular density by immunofluorescent staining of the capillary density using CD31 to identify endothelial cells. As shown in Figure 4a and b, the number of CD31 positive vessels was decreased in the MI group in comparison to the Sham group, and angiogenesis was recovered to some extent by CPC transplantation (122.24 ± 4.03, 82.47 ± 3.59 and 90.33 ± 2.32 per field, Sham, MI and MI + CPC, respectively). The promotion of angiogenesis was even more prominent in the MI + CPC + Irisin group (130.00± 3.40 per field, $p < 0.001$ vs. MI + CPC group).

Irisin pre-treatment attenuates interstitial fibrosis in the infarcted heart after CPC transplantation

Interstitial collagen deposition accompanied by MI in the mouse heart was evaluated with picrosirius red staining. As shown in Figure 5a and b, the fibrotic area was significantly expanded in MI mice as compared to sham-operated group (0.00 ± 0.00 and 5.62 ± 0.57 % total area, Sham and MI, respectively, $p < 0.001$). The MI + CPC group showed a significant reduction of interstitial fibrosis in comparison to MI group (4.73 ± 0.26 % total area, $p < 0.001$ vs. MI), and pre-treatment of the CPCs with irisin-enhanced the anti-fibrotic effects of CPC delivery (1.82 ± 0.31 % total area, $p < 0.001$ vs. MI + CPC).

Irisin pre-treatment promotes proliferation of cardiomyocytes in infarcted area

Ki67 was utilized to determine dividing and amplifying cells. Mitosis was visualized by phosphorylated histone H3 (PH3). Representative images of phospho-histone 3 and Ki-67 staining were shown in Figure 6a and b. As shown in Figure 6c and d, the number of phospho-histone 3 and Ki-67 positive cardiomyocytes was increased in the MI + CPC group as compared to the MI group (phospho-histone 3: 9.8 ± 1.3 and 26.0 ± 4.0 per field, Ki 67: 9.0 ± 1.6 and 24.0 ± 1.4, MI and MI + CPC, respectively, $p < 0.01$). Also, the pro-proliferative effect of CPC transplantation was enhanced in the MI + CPC + Irisin group (phospho-histone 3: 42.0± 3.9 per field, Ki 67: 34.0 ± 3.1 per field, $p < 0.05$ vs. MI + CPC group).

Irisin pre-treatment attenuates apoptosis in infarcted hearts after CPC transplantation

The TUNEL assay was carried out to determine the number of apoptotic myocytes in post-MI hearts. A significant reduction in TUNEL positive myocytes was observed in the infarct sites of MI hearts as compared to the sham control. As shown in Figure 7a, TUNEL positive signals in post-MI hearts that had increased in the MI group were significantly suppressed in the MI + CPC group (1.46% ± 0.26, 9.68 ± 0.34 and 7.10 ± 0.20 total nuclei, Sham, MI and MI + CPC, respectively), and the anti-apoptotic effect was further enhanced in MI + CPC + Irisin group (3.75 %± 0.32 total nuclei, $p < 0.001$ vs. MI + CPC group). Likewise, the percentage of caspase-3 positive cells in infarcted areas also increased in the MI group, but were partially reversed in the MI + CPC group (1.315% ± 0.067, 6.793% ± 0.328, and 4.345% ± 0.149; sham, MI, and MI + CPC, respectively, Figure 7b). The anti-apoptotic effect was enhanced again in the MI + CPC + Irisin group (3.470 %± 0.135, $p < 0.001$ vs. MI + CPC group, Supplemental Figure 4).

The signaling of *in vitro* cultured Nkx2.5^{+} CPCs

In order to see whether irisin treatment could affect apoptosis and cellular signaling of cultured CPCs, we detected the content of active-caspase-3, HDAC4, and p38 acetylation. As shown in Figure 8a, irisin treatment led to the reduction of active-caspase 3 in CPCs exposed to peroxide stress. Irisin treatment also caused HDAC4 inhibition (Figure 8b). Additionally, we have observed an activation of acetylated p38 following irisin treatment (Figure 8c), suggesting that p38 acetylation and HDAC4 inhibition may be involved in irisin-induced cardiogenesis. In addition, we also examined the timeframe of irisin treatment and whether it could affect cell proliferation in the cultured condition.

Discussion

Recent developments in stem cell research provide new approaches in treating MI-induced heart failure by focusing on replacing the damaged myocardium with viable cardiomyocytes. CPCs are shown to have beneficial effects in preventing negative remodeling processes and restoring cardiac function in post-MI hearts (Tao Z et al., 2011; Lange S et al., 2009). However, poor viability (Zhang M et al., 2001; Müller-Ehmsen J et al., 2002) and an inability to regulate the microenvironment of the transplant area detract from the therapeutic potential of stem cells. Identification of new pharmacological approaches holds promise in

developing cell therapies for cardiac repair and MI. This study is the first demonstration that irisin results in cardiac functional improvement and the promotion of cardiac repair.

It was reported that growth factors play an important role in mediating stem cells to induce cardiac repair and achieving protective effects (Harada M et al., 2005; Zhang D et al., 2007; Orlic D et al., 2001; Wang B et al., 2016). Irisin was recently identified as a myokine which is produced by the proteolytic processing of the transmembrane receptor, fibronectin domain-containing protein 5 (FNDC5) (Huh JY et al., 2012; Polyzos SA et al., 2013). It has been proposed that this peptide is secreted during exercise to promote the activity of brown fat cells amongst white adipose tissue to enhance thermogenesis and increase energy expenditure (13). In addition, irisin is produced in numerous other places, including adipose tissue, liver, parotid gland, and cardiac muscles (Huh JY et al., 2012; Kuloglu T et al., 2014; Liu JJ et al., 2013; Roca-Rivada A1 et al., 2013; Anastasilakis AD et al., 2017). In addition, its clinical implications have also been investigated in various pathological disorders (Polyzos SA et al., 2013; Zhang HJ et al., 2013; Stengel A et al., 2013; Sanchis-Gomar F et al., 2012; Vamvini MT et al., 2013; Park KH et al., 2013; Matsuo Y et al., 2015).

In our recent studies, we demonstrated cardioprotective effects of irisin against myocardial ischemia and reperfusion injury (Zhu D et al., 2015; Zhao YT et al., 2016), indicating that irisin plays a critical role in myocardial protection. This study utilized an animal model in order to investigate and delineate the potential therapeutic benefit of irisin in CPC-transplantation for myocardial infarction. The findings here indicate that preconditioning cardiac progenitor cells with irisin enhanced cardiac repair, improved cardiac function, and suppressed myocardial remodeling in cells of engrafted hearts. ESCs are attractive populations for cardiac repair because they can be differentiated into definitive cardiomyocytes. However, teratoma formation has been seen in monkeys injected with unpurified human ESC-derived cardiomyocytes (Nussbaum J et al., 2007). Therefore, the use of a cardiac progenitor cell population is considered to be a superior alternative. Among these identified cardiac progenitor cells, $Nkx2.5^{+}$CPCs have the capacity to form cardiomyocytes, conduction system cells, endothelial cells, and smooth muscle cells (Li G et al., 2015; Musunuru K et al., 2010).

In this study, we have isolated $Nkx2.5^{+}$ CPCs for performing cell transplantation in the infarcted myocardium. Irisin's promotion of cardiac repair was accompanied with an increase in proliferation in cardiomyocytes and other vascular structures in the heart, which was in agreement with the observation in another study in which irisin promoted human umbilical vein endothelial cell proliferation and suppressed high glucose-induced apoptosis (Song H et al., 2014). Our previous works have indicated that HDAC4 plays an important role in modulating c-kit positive CPC-induced cardiac repair (Zhang LX et al., 2014). We found that irisin treatment led to the marked reduction of HDAC4 following irisin treatment, indicating that irisin-treated $Nkx2.5^{+}$ CPC increased myocardial repair was related to HDAC4. Additionally, it was observed that irisin-induced myocardial protection was related to p38 activation. It was reported that p38 was required for the development of cardiogenesis (Yang J et al., 2000). We showed that there was increased p38 acetylation, which was accompanied by the reduction of HDAC4. It will be of interest to define how the molecular signaling is involved in irisin-induced cardiac repair by $Nkx2.5^{+}$CPCs. In addition, post-MI

angiogenesis was also increased following the engraftment of irisin-treated CPCs, which is supported by the evidence that irisin induced angiogenesis in both human umbilical vein endothelial cells and also in zebrafish embryos (Wu F et al., 2015). Increased microvessels following the transplantation of irisin-treated CPCs in MI hearts might also be responsible for the improvement of myocardial function and the reduction of myocardial remodeling. This is supported by observations showing that the augmentation of neovascularization in MI hearts was closely associated with the prevention of cardiac remodeling (Zhang LX et al., 2014; Zhao YT et al., 2015). Since we have also found that irisin induced cardiac protection against myocardial I/R injury, it is also likely that irisin could enhance the paracrine effects of stem cells to repair infarcted hearts (Gnecchi M et al., 2008).

Post MI, the LV undergoes a series of architectural and structural changes along with accelerated fibrosis and collagen deposition, consequently leading to contractile dysfunction and ultimately heart failure. We have previously reported that engraftment of CPCs prevented cardiac remodeling in the murine heart (Zhang LX et al., 2014; Zhao YT et al., 2015). Likewise, we demonstrated the anti-remodeling effect of $Nkx2.5^{+}$ CPCs in which LV hypertrophic changed- features increased individual myocyte size. However, irisin-treated CPCs showed a pronounced effect in attenuating cardiac remodeling and reducing interstitial fibrosis in comparison to CPC transplantation only. In addition to increased cardiomyocyte proliferation elicited by irisin treatment, we also found that transplantation of irisin-treated CPCs resulted in a decrease in apoptotic signals in cell engrafted MI hearts, which might be an important factor for functional improvement in MI hearts receiving irisin treated CPCs. In addition, it is likely that irisin can modify the cytokine profile and metabolism of cultured cells to modulate CPC-derived cardiac repair (Zhang Y et al., 2014; So WY et al., 2014; Li DJ et al., 2017; Lu J et al., 2015; Park MJ et al., 2015), which is of interest for future studies.

Conclusion

Taken together, our results indicate that transplantation of $Nkx2.5^{+}$ CPCs promoted functional restoration, suppressed cardiac hypertrophy, and attenuated remodeling in CSC-engrafted MI hearts. Irisin treatment of $Nkx2.5^{+}$ CPCs enhanced CPC-derived cardiac lineage commitment and proliferation following reintroduction into the MI heart. Furthermore, irisin also increased neovascularization in $Nkx.2.5^{+}$ CPC-engrafted MI myocardium. CPC transplantation in the post-MI heart demonstrated an anti-apoptotic effect in MI hearts, which was augmented by irisin treatment. CPC transplantation displayed an anti-apoptotic effect in MI hearts, which was also augmented by irisin treatment. Our results demonstrate that irisin plays a crucial role in mediating CPCs to induce cardiac regeneration. Our study also holds promise in developing a novel therapeutic approach for cardiac regeneration.

Supplementary Material

Refer to Web version on PubMed Central for supplementary material.

Acknowledgments

The work is supported by the National Heart, Lung, and Blood Institute Grants (R01 HL089405 and R01 HL115265).

References

Aydin S, Aydin S, Kobat MA, Kalayci M, Eren MN, Yilmaz M, Kuloglu T, Gul E, Secen O, Alatas OD, Baydas A. 2014; Decreased saliva/serum irisin concentrations in the acute myocardial infarction promising for being a new candidate biomarker for diagnosis of this pathology. Peptides. 56:141–5. [PubMed: 24747283]

Anastasilakis CD, Mantzoros CS. 2017; Circulating irisin levels are lower in patients with either stable coronary artery disease (CAD) or myocardial infarction (MI) versus healthy controls, whereas follistatin and activin A levels are higher and can discriminate MI from CAD with similar to CK-MB accuracy. Metabolism. 73:1–8. [PubMed: 28732565]

Boström P, Wu J, Jedrychowski MP, Korde A, Ye L, Lo JC, Spiegelman BM. 2012; A PGC1-α-dependent myokine that drives brown-fat-like development of white fat and thermogenesis. Nature. 481:463–8. [PubMed: 22237023]

Chen HP, Denicola M, Qin X, Zhao Y, Zhang L, Long XL, Zhuang S, Liu PY, Zhao TC. 2011; HDAC inhibition promotes cardiogenesis and the survival of embryonic stem cells through proteasome-dependent pathway. J Cell Biochem. 112:3246–55. [PubMed: 21751234]

Finegold JA, Asaria P, Francisa DP. 2013; Mortality from ischaemic heart disease by country, region, and age: Statistics from World Health Organisation and United Nations. Int J Cardiol. 168:934–945. [PubMed: 23218570]

Gnecchi M, Zhang Z, Ni A, Dzau VJ. 2008; Paracrine mechanisms in adult stem cell signaling and therapy. Circ Res. 103:1204–19. [PubMed: 19028920]

Harada M, Qin Y, Takano H, Minamino T, Zou Y, Toko H, Ohtsuka M, Matsuura K, Sano M, Nishi J, Iwanaga K, Akazawa H, Kunieda T, Zhu W, Hasegawa H, Kunisada K, Nagai T, Nakaya H, Yamauchi-Takihara K, Komuro I. 2005; G-CSF prevents cardiac remodeling after myocardial infarction by activating the Jak-Stat pathway in cardiomyocytes. Nat Med. 11:305–11. [PubMed: 15723072]

Hu W, Wang R, Li J, Zhang J, Wang W. 2016; Association of irisin concentrations with the presence of diabetic nephropathy and retinopathy. Ann ClinBiochem. 53:67–74.

Huh JY, Panagiotou G, Mougios V, Brinkoetter M, Vamvini MT, Schneider BE, Mantzoros CS. 2012; FNDC5 and irisin in humans: I. Predictors of circulating concentrations in serum and plasma and II. mRNA expression and circulating concentrations in response to weight loss and exercise. Metabolism. 61:1725–38. [PubMed: 23018146]

Jeremic N, Chatuverdi P, Tyagi SC. 2017; Browning of white fat: Novel insight into factors, mechanisms and therapeutics. J Cell Physiol. 232:61–8. [PubMed: 27279601]

Kuloglu T, Aydin S, Eren MN, Yilmaz M, Sahin I, Kalayci M, Sarman E, Kaya N, Yilmaz OF, Turk A, Aydin Y, Yalcin MH, Uras N, Gurel A, Ilhan S, Gul E, Aydin S. 2014; Irisin: a potentially candidate marker for myocardial infarction. Peptides. 55:85–91. [PubMed: 24576483]

Lange S, Heger J, Euler G, Wartenberg M, Piper HM, Sauer H. 2009; Platelet-derived growth factor BB stimulates vasculogenesis of embryonic stem cell-derived endothelial cells by calciummediated generation of reactive oxygen species. Cardiovasc Res. 81:159–68. [PubMed: 18806276]

Laugwitz KL, Moretti A, Lam J, Gruber P, Chen Y, Woodard S, Lin LZ, Cai CL, Lu MM, Reth M, Platoshyn O, Yuan JX, Evans S, Chien KR. 2005; Postnatal isl1+ cardioblasts enter fully differentiated cardiomyocyte lineages. Nature. 433:647–53. [PubMed: 15703750]

Li DJ, Li YH, Yuan HB, Qu LF, Wang P. 2017; The novel exercise-induced hormone irisin protects against neuronal injury via activation of the Akt and ERK1/2 signaling pathways and contributes to the neuroprotection of physical exercise in cerebral ischemia. Metabolism. 68:31–42. [PubMed: 28183451]

Li G, Plonowska K, Kuppusamy R, Sturzu A, Wu SM. 2015; Identification of cardiovascular lineage descendants at single-cell resolution. Development. 142:846–57. [PubMed: 25633351]

Liu JJ, Wong MD, Toy WC, Tan CS, Liu S, Ng XW, Tavintharan S, Sum CF, Lim SC. 2013; Lower circulating irisin is associated with type 2 diabetes mellitus. J Diabetes Complications. 27:365–9. [PubMed: 23619195]

Lu J, Xiang G, Liu M, Mei W, Xiang L, Dong J. 2015; Irisin protects against endothelial injury and ameliorates atherosclerosis in apolipoprotein E-Null diabetic mice. Atherosclerosis. 243:438–48. [PubMed: 26520898]

Matsuo Y, Gleitsmann K, Mangner N, Werner S, Fischer T, Bowen TS, Kricke A, Matsumoto Y, Kurabayashi M, Schuler G, Linke A, Adams V. 2015; Fibronectin type III domain containing 5 expression in skeletal muscle in chronic heart failure—relevance of inflammatory cytokines. J Cachexia Sarcopenia Muscle. 6:62–72. [PubMed: 26136413]

Menasché P, Vanneaux V, Fabreguettes JR, Bel A, Tosca L, Garcia S, Bellamy V, Farouz Y, Pouly J, Damour O, Périer MC, Desnos M, Hagège A, Agbulut O, Bruneval P, Tachdjian G, Trouvin JH, Larghero J. 2015; Towards a clinical use of human embryonic stem cell-derived cardiac progenitors: a translational experience. Eur Heart J. 36:743–50. [PubMed: 24835485]

Müller-Ehmsen J, Whittaker P, Kloner RA, Dow JS, Sakoda T, Long TI, Laird PW, Kedes L. 2002; Survival and development of neonatal rat cardiomyocytes transplanted into adult myocardium. J Mol Cell Cardiol. 34:107–16. [PubMed: 11851351]

Musunuru K, Domian IJ, Chien KR. 2010; Stem cell models of cardiac development and disease. Annu Rev Cell Dev Biol. 26:667–687. [PubMed: 20604707]

Nussbaum J, Minami E, Laflamme MA, Virag JA, Ware CB, Masino A, Muskheli V, Pabon L, Reinecke H, Murry CE. 2007; Transplantation of undifferentiated murine embryonic stem cells in the heart: teratoma formation and immune response. FASEB J. 21:1345–57. [PubMed: 17284483]

Oh H, Bradfute SB, Gallardo TD, Nakamura T, Gaussin V, Mishina Y, Pocius J, Michael LH, Behringer RR, Garry DJ, Entman ML, Schneider MD. 2003; Cardiac progenitor cells from adult myocardium: homing, differentiation, and fusion after infarction. Proc Natl AcadSci U S A. 100:12313–8.

Orlic D, Kajstura J, Chimenti S, Bodine DM, Leri A, Anversa P. 2001; Transplanted adult bone marrow cells repair myocardial infarcts in mice. Ann NY Acad Sci. 938:221–9. [PubMed: 11458511]

Park KH, Zaichenko L, Brinkoetter M, Thakkar B, Sahin-Efe A, Joung KE, Tsoukas MA, Geladari EV, Huh JY, Dincer F, Davis CR, Crowell JA, Mantzoros CS. 2013; Circulating irisin in relation to insulin resistance and the metabolic syndrome. J Clin Endocrinol Metab. 98:4899–907. [PubMed: 24057291]

Park MJ, Kim DI, Choi JH, Heo YR, Park SH. 2015; New role of irisin in hepatocytes: The protective effect of hepatic steatosis in vitro. Cell Signal. 27:1831–9. [PubMed: 25917316]

Polyzos SA, Kountouras J, Shields K, Mantzoros CS. 2013; Irisin: A renaissance in metabolism? Metabolism. 62:1037–44. [PubMed: 23664085]

Qiao H, Zhang H, Yamanaka S, Patel VV, Petrenko NB, Huang B, Muenz LR, Ferrari VA, Boheler KR, Zhou R. 2011; Long-term improvement in postinfarct left ventricular global and regional contractile function is mediated by embryonic stem cell-derived cardiomyocytes. Circ Cardiovasc luImag. 4:33–41.

Roca-Rivada A, Castelao C, Senin LL, Landrove MO, Baltar J, BelénCrujeiras A, Seoane LM, Casanueva FF, Pardo M. 2013; FNDC5/irisin is not only a myokine but also an adipokine. PLoS One. 8:e60563. [PubMed: 23593248]

Sanchis-Gomar F, Lippi G, Mayero S, Perez-Quilis C, García-Giménez JL. 2012; Irisin: a new potential hormonal target for the treatment of obesity and type 2 diabetes. J Diabetes. 4:196. [PubMed: 22372821]

Song H, Wu F, Zhang Y, Zhang Y, Wang F, Jiang M, Wang Z, Zhang M, Li S, Yang L, Wang XL, Cui T, Tang D. 2014; Irisin promotes human umbilical vein endothelial cell proliferation through the ERK signaling pathway and partly suppresses high glucose-induced apoptosis. PLoS One. 9:e110273. [PubMed: 25338001]

So WY, Leung PS. 2016; Irisin ameliorates hepatic glucose/lipid metabolism and enhances cell survival in insulin-resistant human HepG2 cells through adenosine monophosphate-activated protein kinase signaling. Int J Biochem Cell Biol. 78:237–47. [PubMed: 27452313]

Stamm C, Westphal B, Kleine HD, Petzsch M, Kittner C, Klinge H, Schümichen C, Nienaber CA, Freund M, Steinhoff G. 2003; Autologous bone-marrow stem-cell transplantation for myocardial regeneration. Lancet. 361:45–6. [PubMed: 12517467]

Stengel A, Hofmann T, Goebel-Stengel M, Elbelt U, Kobelt P, Klapp BF. 2013; Circulating levels of irisin in patients with anorexia nervosa and different stages of obesity–correlation with body mass index. Peptides. 39:125–30. [PubMed: 23219488]

Tao Z, Chen B, Tan X, Zhao Y, Wang L, Zhu T, Cao K, Yang Z, Kan YW, Su H. 2011; Coexpression of VEGF and angiopoietin-1 promotes angiogenesis and cardiomyocyte proliferation reduces apoptosis in porcine myocardial infarction (MI) heart. Proc Natl Acad Sci. 108:2064–9. [PubMed: 21245320]

Vamvini MT, Aronis KN, Panagiotou G, Huh JY, Chamberland JP, Brinkoetter MT, Petrou M, Christophi CA, Kales SN, Christiani DC, Mantzoros CS. 2013; Irisin mRNA and circulating levels in relation to other myokines in healthy and morbidly obese humans. Eur J Endocrinol. 169:829–34. [PubMed: 24062354]

Wang B, Ma X, Zhao L, Zhou X, Ma Y, Sun H, Yang Y, Chen B. 2016; Injection of basic fibroblast growth factor together with adipose-derived stem cell transplantation: improved cardiac remodeling and function in myocardial infarction. ClinExp Med. 16:539–50.

Wang H, Zhao YT, Zhang S, Dubielecka PM, Du J, Yano N, Chin YE, Zhuang S, Qin G, Zhao TC. 2017; Irisin plays a pivotal role to protect the heart against ischemia and reperfusion injury. J Cell Physiol. 232:3775–85. [PubMed: 28181692]

Westrich J, Yaeger P, He C, He C, Stewart J, Chen R, Seleznik G, Larson S, Wentworth B, O'Callaghan M, Wadsworth S, Akita G, Molnar G. 2010; Factors affecting residence time of mesenchymal stromal cells (MSC) injected into the myocardium. Cell Transplant. 19:937–48. [PubMed: 20350355]

Wu F, Song H, Zhang Y, Zhang Y, Mu Q, Jiang M, Wang F, Zhang W, Li L, Li H, Wang Y, Zhang M, Li S, Yang L, Meng Y, Tang D. 2015; Irisin Induces Angiogenesis in Human Umbilical Vein Endothelial Cells In Vitro and in Zebrafish Embryos In Vivo via Activation of the ERK Signaling Pathway. PLoS One. 10:e0134662. [PubMed: 26241478]

Yang J, Boerm M, McCarty M, Bucana C, Fidler IJ, Zhuang Y, Su B. 2000; Mekk3 is essential for early embryonic cardiovascular development. Nat Genet. 24:309–13. [PubMed: 10700190]

Zhang D, Zhang F, Zhang Y, Gao X, Li C, Yang N, Cao K. 2007; Combining erythropoietin infusion with intramyocardial delivery of bone marrow cells is more effective for cardiac repair. Transplant Int. 20:174–83.

Zhang D, Huang W, Dai B, Zhao T, Ashraf A, Millard RW, Ashraf M, Wang Y. 2010; Genetically manipulated progenitor cell sheet with diprotin A improves myocardial function and repair of infarcted hearts. Am J Physiol Heart Circ Physiol. 299:H1339–47. [PubMed: 20802132]

Zhang G, Wang X, Wang Z, Zhang J, Suggs L. 2006; A PEGylated fibrin patch for mesenchymal stem cell delivery. Tissue Eng. 12:9–19. [PubMed: 16499438]

Zhang HJ, Zhang XF, Ma ZM, Pan LL, Chen Z, Han HW, Han CK, Zhuang XJ, Lu Y, Li XJ, Yang SY, Li XY. 2013; Irisin is inversely associated with intrahepatic triglyceride contents in obese adults. J Hepatol. 59:557–62. [PubMed: 23665283]

Zhang S, Jia Z, Ge J, Gong L, Ma Y, Li T, Guo J, Chen P, Hu Q, Zhang P, Liu Y, Li Z, Ma K, Li L, Zhou C. 2005; Purified human bone marrow multipotent mesenchymal stem cells regenerate infarcted myocardium in experimental rats. Cell Transplant. 14:787–98. [PubMed: 16454353]

Zhang LX, DeNicola M, Qin X, Du J, Ma J, Tina Zhao Y, Zhuang S, Liu PY, Wei L, Qin G, Tang Y, Zhao TC. 2014; Specific inhibition of HDAC4 in cardiac progenitor cells enhances myocardial repairs. Am J Physiol Cell Physiol. 307:C358–72. [PubMed: 24944198]

Zhang L, Chen B, Zhao Y, Dubielecka PM, Wei L, Qin GJ, Chin YE, Wang Y, Zhao TC. 2012; Inhibition of histone deacetylase-induced myocardial repair is mediated by c-kit in infarcted hearts. J Biol Chem. 287:39338–48. [PubMed: 23024362]

Zhang M, Methot D, Poppa V, Fujio Y, Walsh K, Murry CE. 2001; Cardiomyocyte grafting for cardiac repair: graft cell death and anti-death strategies. J Mol Cell Cardiol. 33:907–21. [PubMed: 11343414]

Zhao M, Barron MR, Li Z, Koprowski S, Hall CL, Lough J. 2010; Making stem cells infarct avid. Cell Transplant. 19:245–50. [PubMed: 19878624]

Zhao TC, Cheng G, Zhang LX, Tseng YT, Padbury JF. 2007; Inhibition of histone deacetylases triggers pharmacologic preconditioning effects against myocardial ischemic injury. Cardiovasc Res. 76:473–81. [PubMed: 17884027]

Zhang Y, Li R, Meng Y, Li S, Donelan W, Zhao Y, Qi L, Zhang M, Wang X, Cui T, Yang LJ, Tang D. 2014; Irisin stimulates browning of white adipocytes through mitogen-activated protein kinase p38 MAP kinase and ERK MAP kinase signaling. Diabetes. 63:514–25. [PubMed: 24150604]

Zhao YT, Wang H, Zhang S, Du J, Zhuang S, Zhao TC. 2016; Irisin Ameliorates Hypoxia/Reoxygenation-Induced Injury through Modulation of Histone Deacetylase 4. PLoS One. 11:e0166182. [PubMed: 27875543]

Zhao YT, Du J, Chen Y, Tang Y, Qin G, Lv G, Zhuang S, Zhao TC. 2015; Inhibition of Oct 3/4 mitigates the cardiac progenitor-derived myocardial repair in infarcted myocardium. Stem Cell Res Ther. 6:259. [PubMed: 26704423]

Zhu D, Wang H, Zhang J, Zhang X, Xin C, Zhang F. 2015; Irisin improves endothelial function in type 2 diabetes through reducing oxidative/nitrative stresses. J Mol Cell Cardiol. 87:138–47. [PubMed: 26225842]

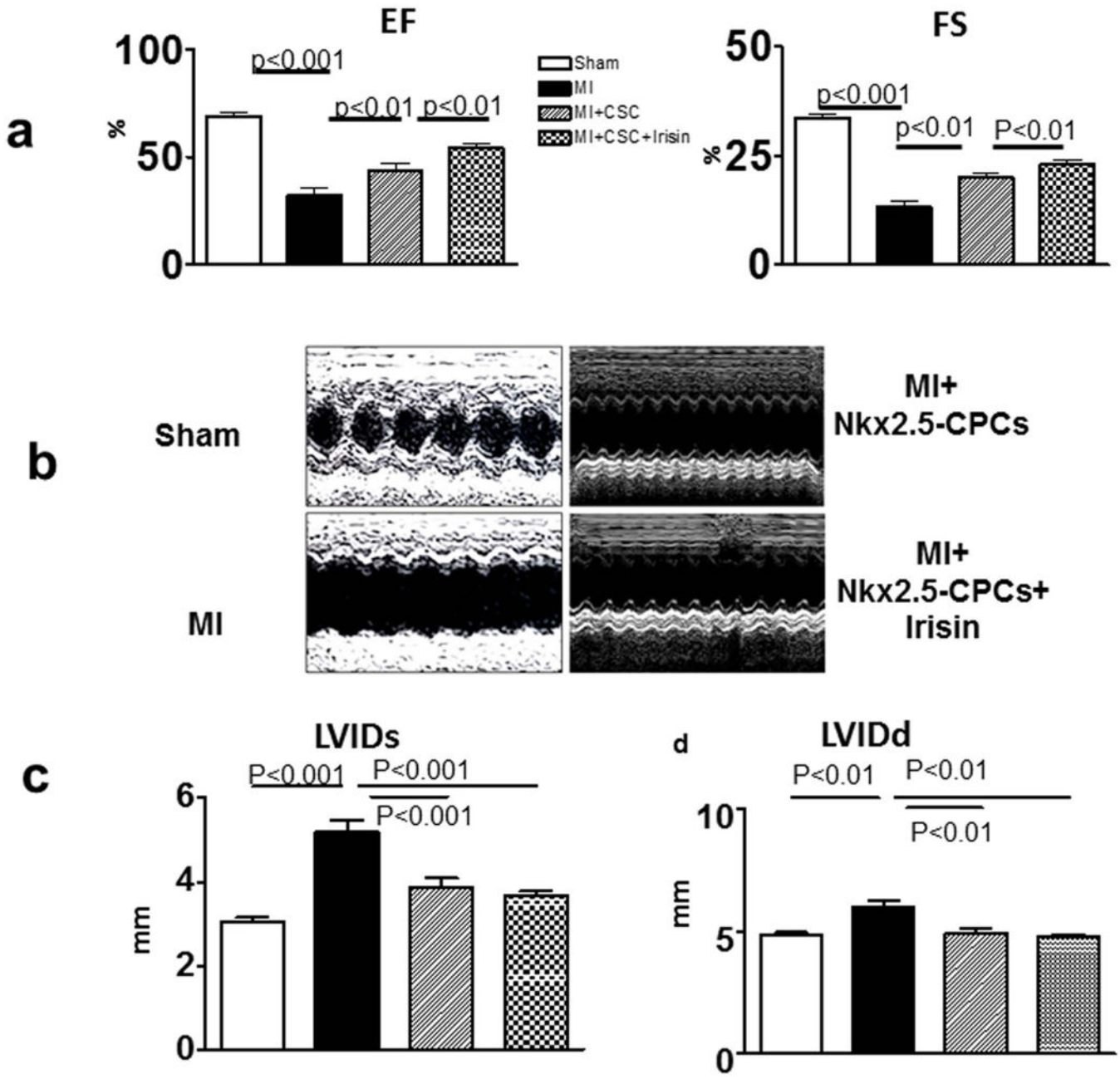

Figure 1. Echocardiographic measurements of ventricular function

(a) Echocardiographic measurements of ventricular functional parameter: ejection fraction (EF) and fractional shortening (FS). (b) Representative images are shown as the M-mode short-axis ultrasound among groups. (c and d): Left ventricular internal diameter at systole (LVIDs) and left ventricular internal diameter at diastole (LVIDd). Values represent mean ± SE (n = 4 – 7/per group).

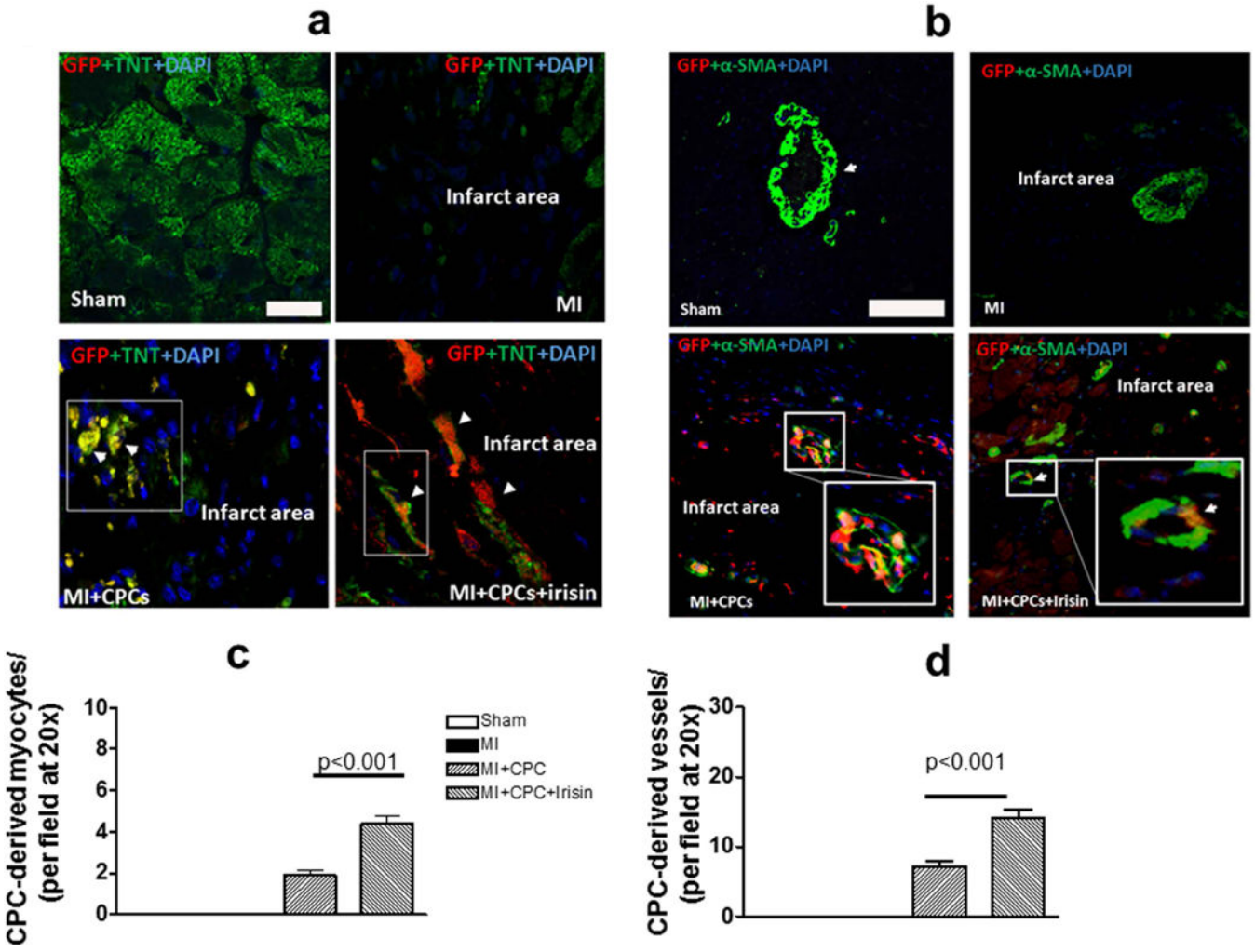

Figure 2. Irisin pre-treatment promotes differentiations of CPCs into cardiomyocytes and smooth-muscle cells of vessels

(a) Representative images showing localization of CPC derived cardiomyocytes in MI receiving CPC treatments among groups (GFP, troponin T double positive cells); TNT: troponin T; scale bars in pictures indicate 10 μm. (b) Representative images showing localization and comparison of the CPC derived smooth muscle of vessels in MI receiving CPC treatments among groups (GFP, SMA double positive cells); scale bars in pictures indicate 100 μm. (c) Quantification of CPC derived cardiomyocytes in the infarcted area. (d) Quantification of CPC derived smooth muscle cells of vessels in the infarcted area. Values in the bar graphs represent means ± SE (n = 4-5 hearts/per group).

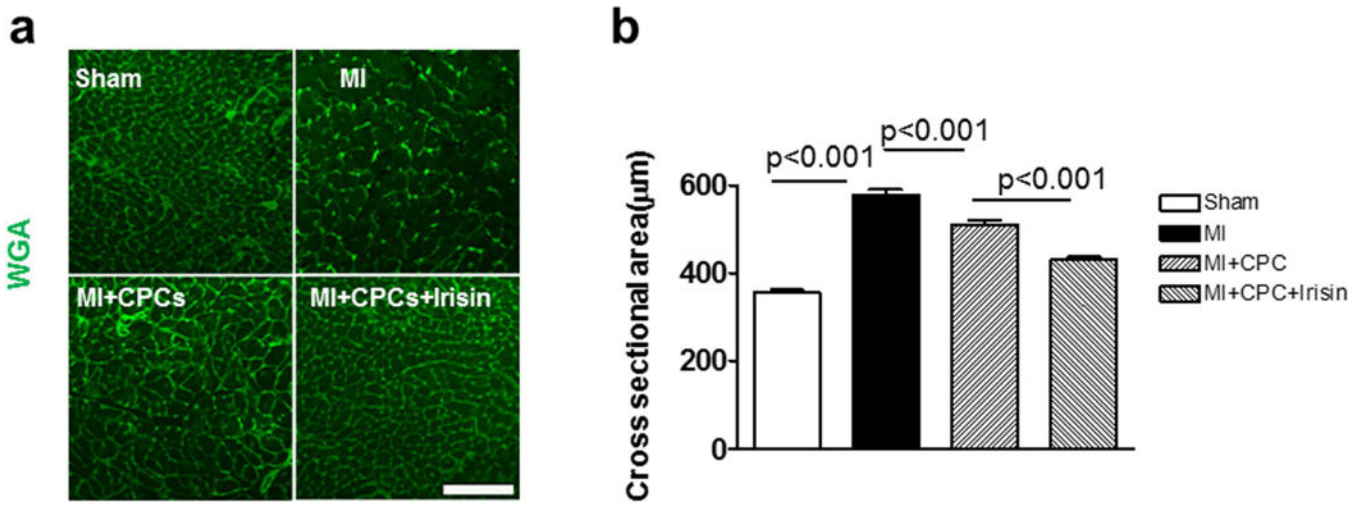

Figure 3. Irisin attenuates hypertrophy of cardiomyocytes due to ischemic damages

(a) Representative image of WGA staining of cardiomyocytes from sham, MI, MI + CPC, and MI + CPC + irisin group of mice. (b) A graph for cross sectional areas of each group. Values represent means ± SE. Scale bars in pictures indicate 100 μm. (n = 4 – 5/per group).

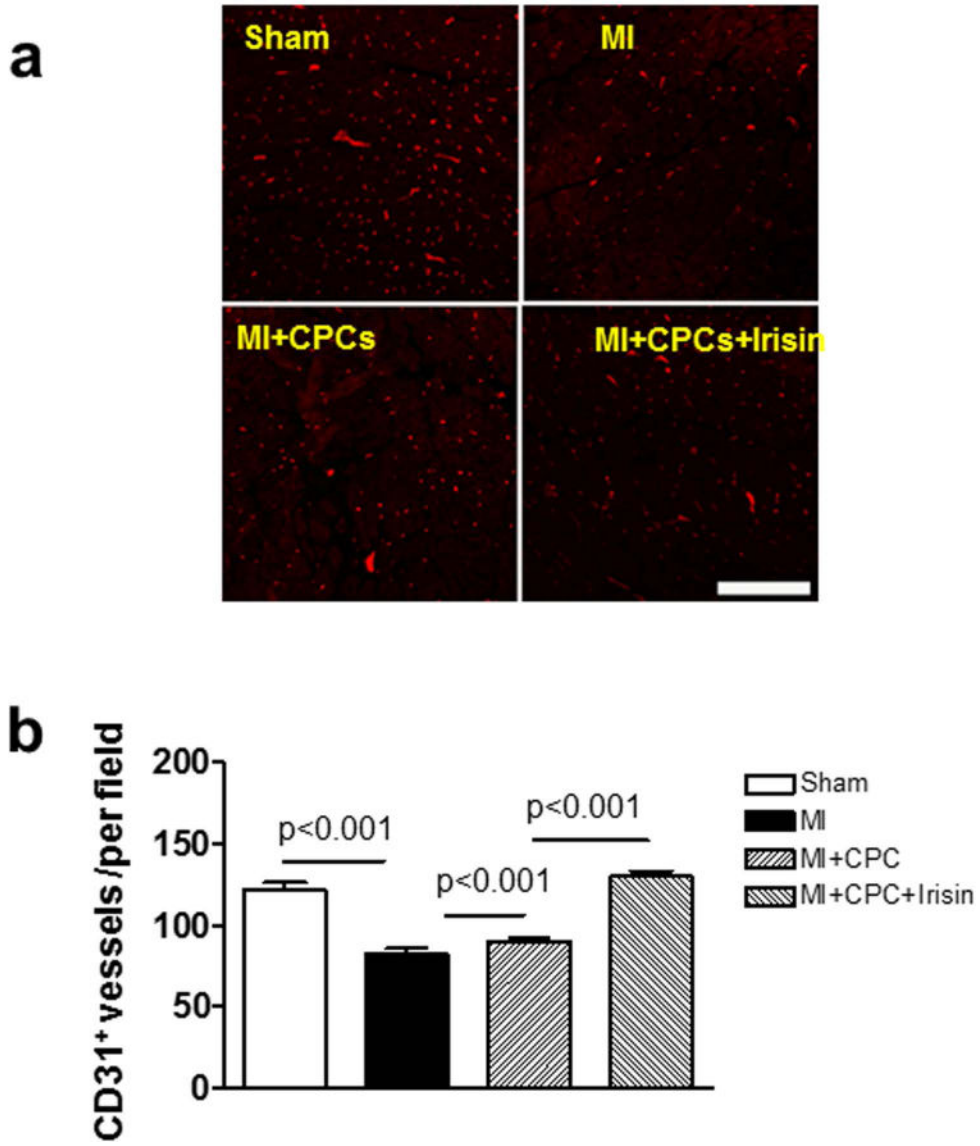

Figure 4. Irisin promotes angiogenesis after CPC transplantation in infarcted heart

(a) Representative image of CD31 of vessel endothelial cells in sham, MI, MI + CPC, and MI + CPC + irisin group of mice. Scale bars in picture indicate 100 μm. (b) A graph for the number of CD31 positive cells in the infarcted heart. Values represent means ± SE. (n = 4 – 5/per group).

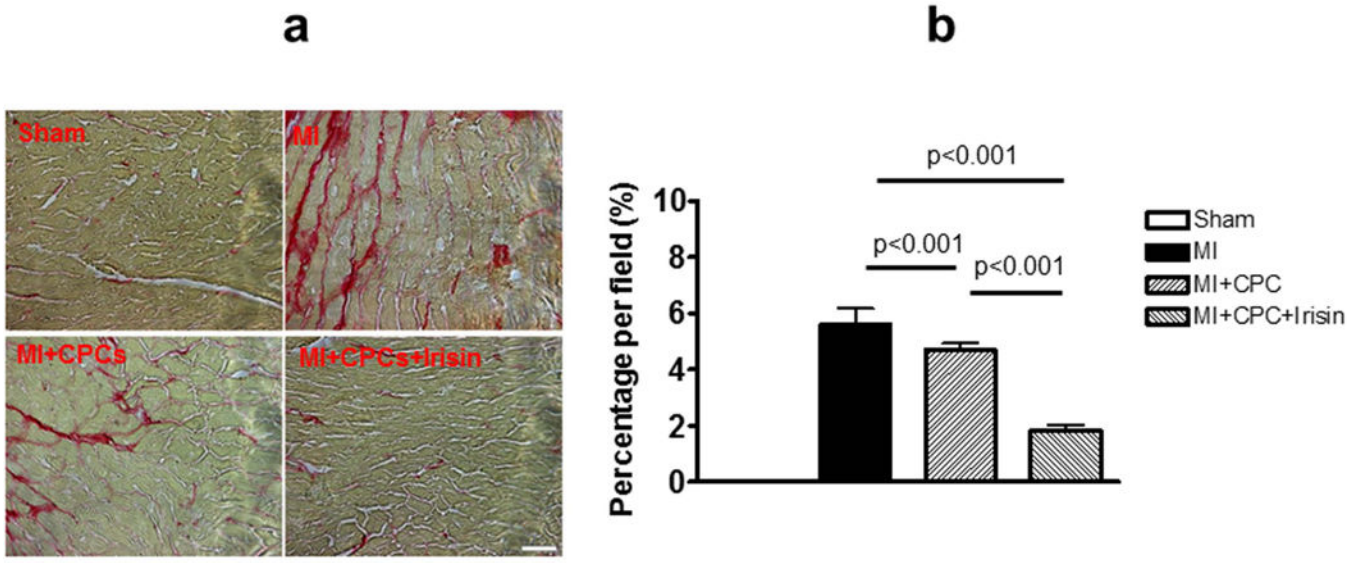

Figure 5. Comparison of interstitial fibrosis deposition in MI hearts

(a) Representative images showing picrosirius red staining in sham, MI, MI + PCP, and MI + CPC + irisin group mice. Scale bars in picture indicates 100 μm. (b) Quantitative analysis of interstitial fibrotic area. Values represent mean ± SE. (n = 3-5/per group).

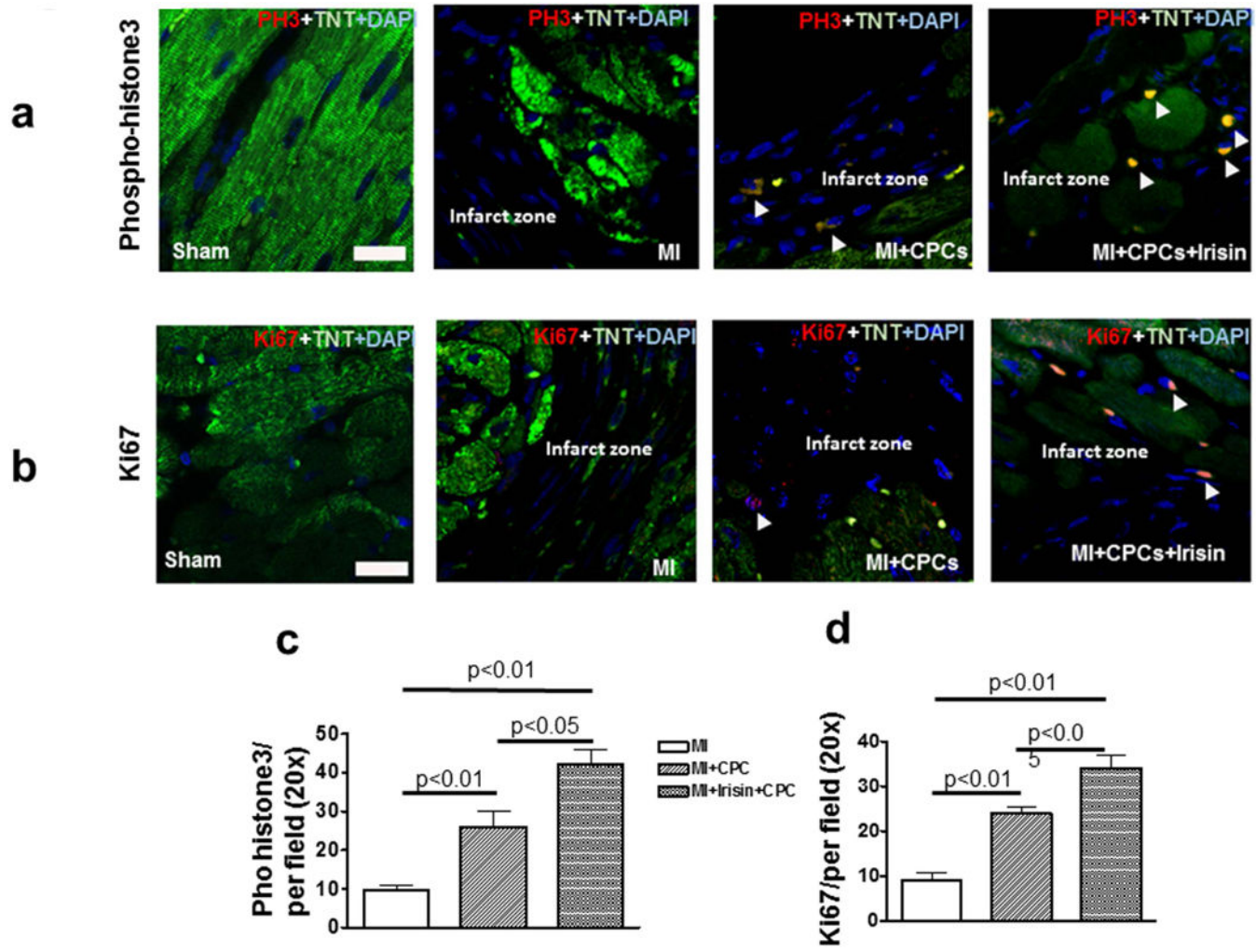

Figure 6. Dual immunofluorescent staining of phospho-histone 3 and Ki67 with cardiomyocyte

Representative images of phospho-histone 3 (a) and Ki67 (b) staining in MI, MI + PCP, and MI + CPC + irisin group mice. Scale bars in picture indicate 10μm. Quantitative analysis of the numbers of phospho-histone 3 positive cells (c) and Ki67 positive cells (d) per field, TNT: troponin T. Values represent mean ± SE. (n = 4-5/per group).

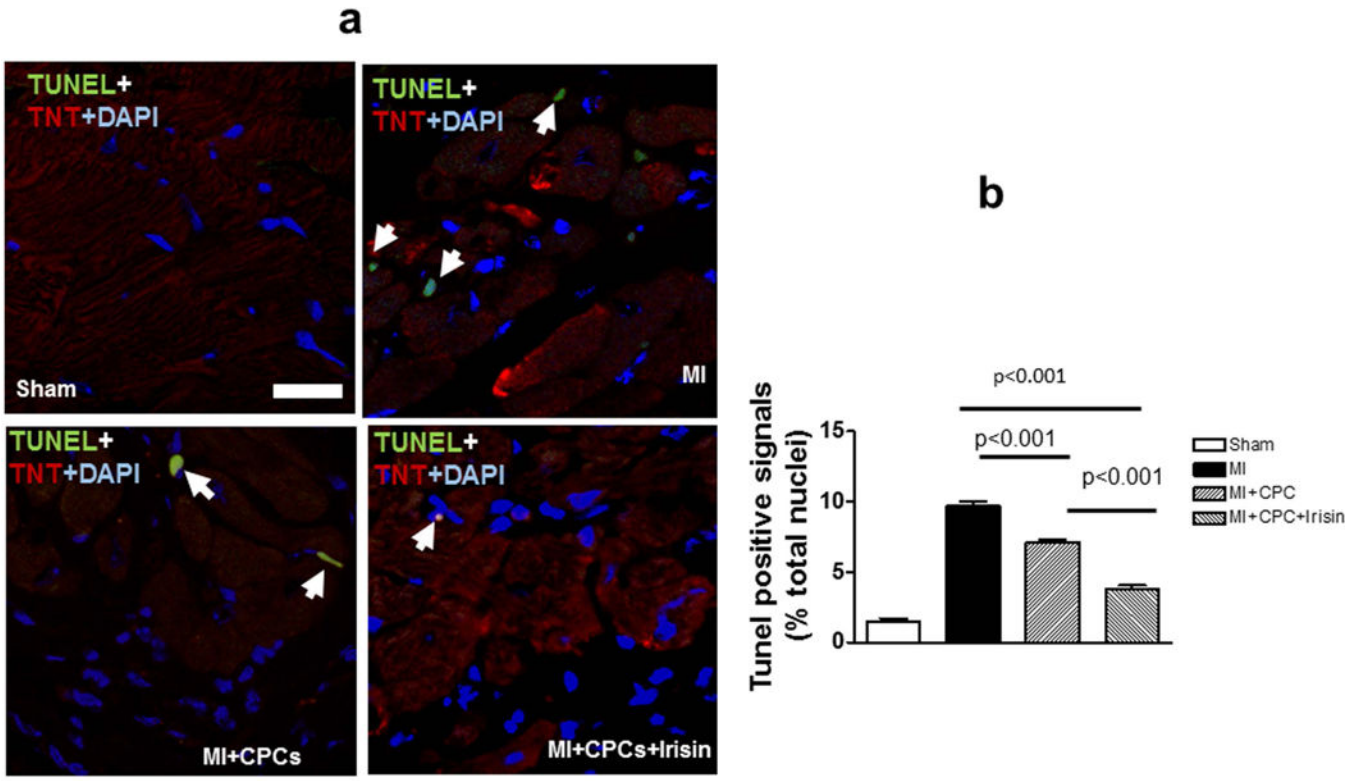

Figure 7. Irisin attenuated apoptotic myocytes in CPC-engrafted MI heart

a: Representative images of TUNEL staining (Green: TUNEL positive staining; red: troponin T; blue: DAPI); b: Quantitative analysis of TUNEL positive signals in the post-MI heart. Values are shown as mean ± SEM (n = 3-5 per group). Scale bar: 10μm

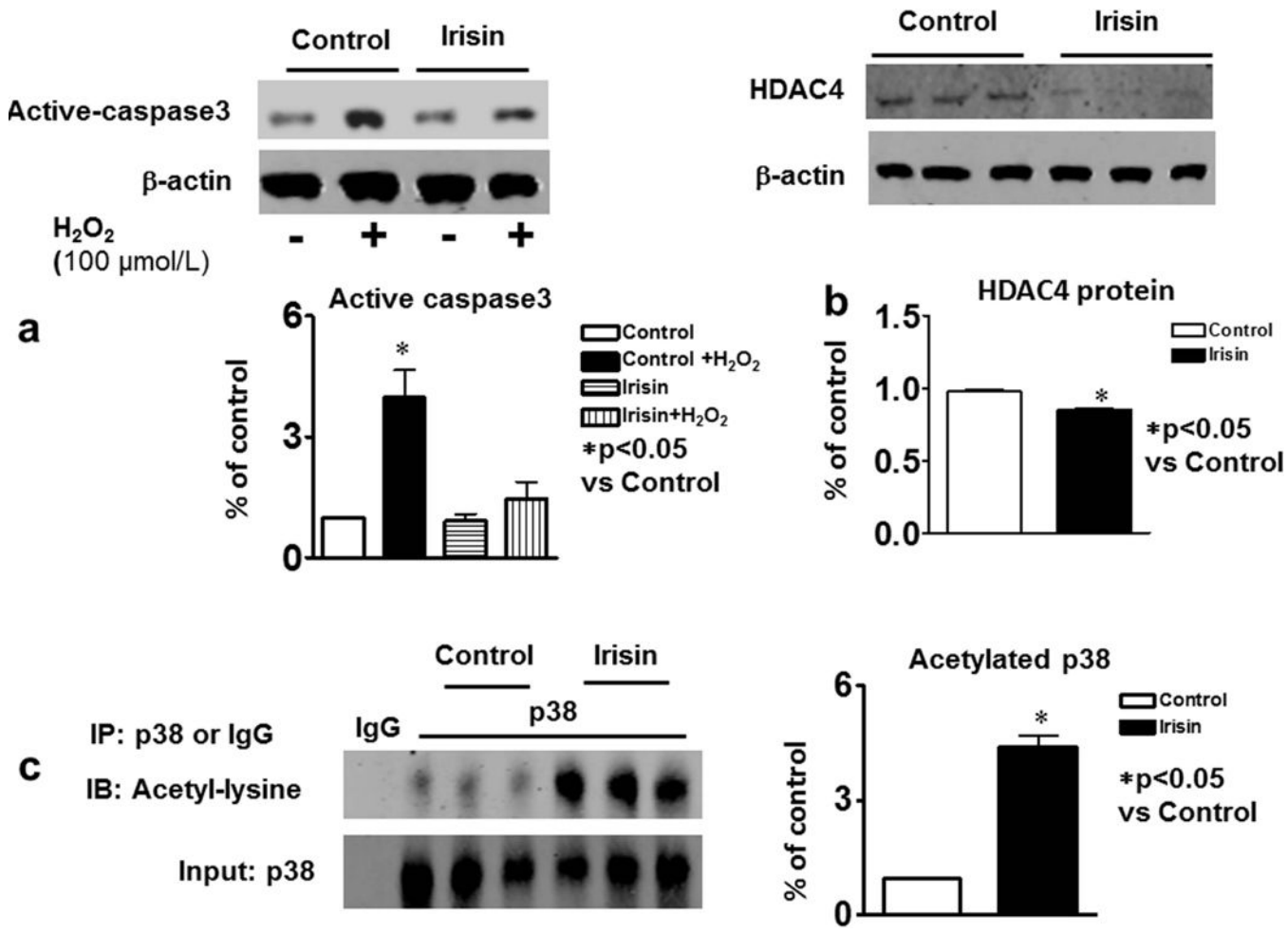

Figure 8. Western blot showing active caspase 3, HDAC4 and acetylated p38 in Nkx2.5^{+}CPCs

(a) Representative Western blot showing the effect of irisin on the content of active caspase 3 and quantification of densitometry of gels among individual groups (n=3 per group), Values are shown as mean ± SEM, *p<0.05 vs control group; (b) Representative Western blot showing the effect of irisin on the content of HDAC4 and densitometry of gels among individual groups (n=3 per group),; *p<0.05 vs control group; (c) Representative Western blot showing the effect of irisin on the content of acetylated p38 and quantification of densitometry of gels among individual groups (n=3 per group), *p<0.05 vs control group; IgG serves as control.

Table 1

Echocardiographie measurement of ventricular functions at baseline.

	Sham	MI	MI+CPCs	MI+CPCs+Irisin
LVIDd (mm)	4.20 ± 0.15	4.18±0.04	4.06±0.08	4.40±0.09
LMDs (mm)	2.92±0.07	3.08 ± 0.10	2.76 ± 0.12	3.24 ± 0.04
EF (%)	64.16 ± 1.95	59.06±2.93	67.12±3.71	57.96±2.76
FS (%)	30.04 ± 1.29	26.9 ± 1.81	32.44±2.54	26.28 ± 1.79

LVIDd: Left Ventricular Internal Dimension in end-diastole; LVIDs: Left Ventricular Internal Dimension in end-systole; EF: Ejection Fraction; FS: Fraction Shortening; Values represent mean ± SE (N=4-7 per group).